

Supporting Information

Nano-graphite Functionalized Mesocellular Carbon Foam with Enhanced Intra-penetrating Electrical Percolation Networks for High Performance Electrochemical Energy Storage Electrode Materials

Changshin Jo,^{‡a} Sunhyung An,^{‡a} Younghoon Kim,^b Jongmin Shim,^a Songhun Yoon,^{*b} and Jinwoo Lee^{*a}

^aDepartment of Chemical Engineering, Pohang University of Science and Technology, Hyo-ja dong, Pohang, Kyungbuk, 790-784, KOREA. ^bGreen Chemical Technology Division, Korea Research Institute of Chemical Technology (KRICT), Daejeon, 305-600, KOREA, [‡] Both authors contributed equally to this work

E-mail address: jinwoo03@postech.ac.kr, yoonsun@kRICT.re.kr

Table S1. EDLC performance of various mesoporous carbon materials.

Type of carbons	Surface area/ $\text{m}^2 \text{g}^{-1}$	Capacitance / F g^{-1}	Electrolyte	Reference
SOMC (Short pore length ordered mesoporous carbon)	1179 (3.9 nm pores)	127 (at 5 mV s^{-1})	6 M KOH	H.-Q. Li et al. <i>J. Electrochem. Soc.</i> , 154, A731 (2007)
LOMC (Long pore length ordered mesoporous carbon)	1362 (3.8 nm pores)	113 (at 5 mV s^{-1})	6 M KOH	H.-Q. Li et al. <i>J. Electrochem. Soc.</i> , 154, A731 (2007)
CMK-3 (Mesoporous carbon, 2-dimensional hexagonal structure)	984 (4 nm pores)	115 (at 2 mV s^{-1})	6 M KOH	K. Xia et al. <i>Carbon</i> , 46, 1718 (2008)
MSU-F-C (Mesocellular carbon)	928 (4 & 28nm pores)	109 (at 4 mV s^{-1})	2 M H_2SO_4	This work
MSU-F-C-G (Graphite functionalized mesocellular carbon)	394 (28 nm pores)	93 (at 4 mV s^{-1})	2 M H_2SO_4	This work

Table S2. Lithium ion battery anode performance of mesoporous carbon materials.

Type of carbons	Surface area/ $\text{m}^2 \text{g}^{-1}$	Reversible capacity / mAh g^{-1}	ΔV	Initial coulombic efficiency / % (ratio of discharge/charge)	Reference
Tir-OMC (Mesoporous carbon, 2-dimensional hexagonal structure)	2390 (6.7 nm pores)	1048 (500 mAh g^{-1} after 50 cycles)	0.01 - 3	34	H.-Q. Li et al. <i>Carbon</i> 45, 2628 (2007)
CMK-3 (Mesoporous carbon, 2-dimensional hexagonal structure)	1147 (4 nm pores)	1100 – 850 in 20 cycles	0.01 - 3	34	H. Zhou et al. <i>Adv. Mater.</i> , 15, 2107 (2003)
MSU-F-C (Mesocellular carbon)	928 (4 & 28nm pores)	624 (99 % retention after 50 cycles)	0 – 2.5	27.5	This work
MSU-F-C-G (Graphite functionalized mesocellular carbon)	394 (28 nm pores)	581 (93 & retention after 50 cycles)	0 – 2.5	43.6	This work

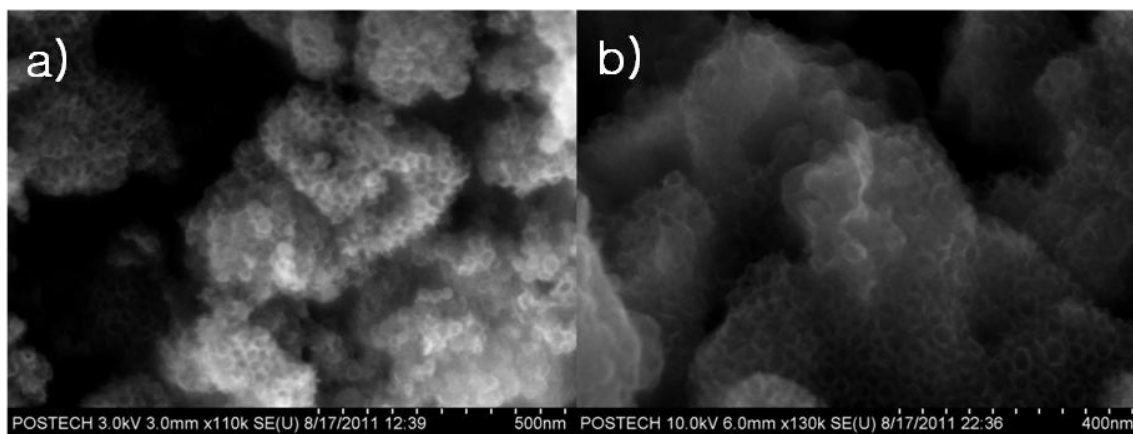


Figure S1. SEM images of (a) MSU-F-C and (b) MSU-F-C-G. The particle shape did not change after functionalization of the nanographite on MSU-F-C.

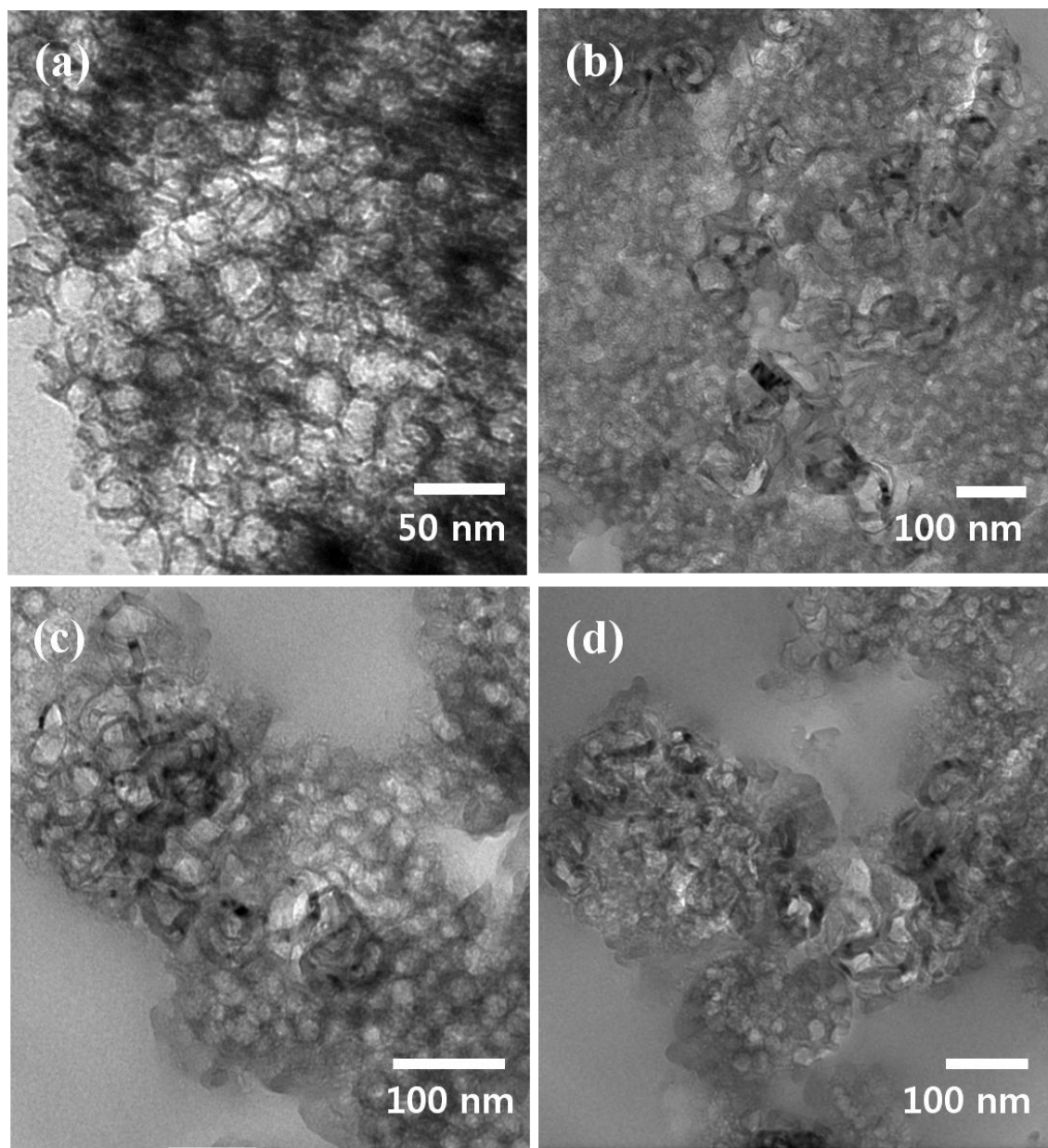


Figure S2. TEM images of (a) MSU-F-C and (b)-(d) MSU-F-C-G.

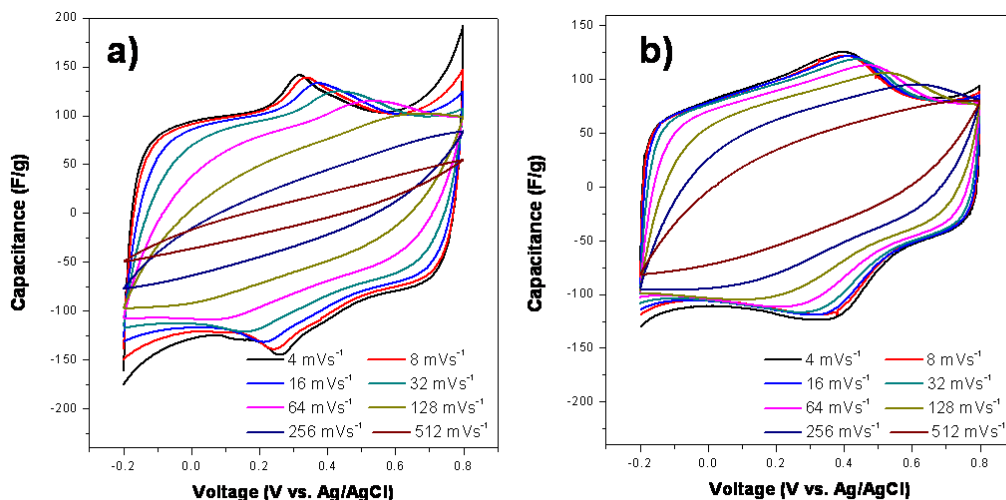


Figure S3. Capacitance-voltage profiles of (a) MSU-F-C and (b) MSU-F-C-G obtained from cyclic voltammograms. The large time constant ($\tau = ESR \times C$) of the MSU-F-C electrode distorts the rectangular shaped response of the current under high scan rate conditions. On the other hand, the enhanced electrical conductivity of the MSU-F-C-G material results in a better capacitance retention under high scan rate conditions.

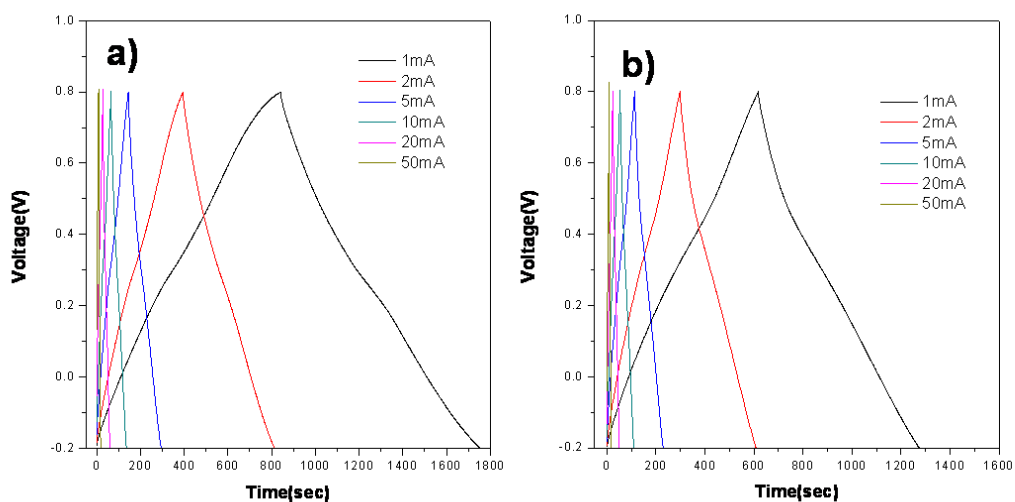


Figure S4. Galvanostatic charge/discharge graphs of (a) MSU-F-C, and (b) MSU-F-C-G within the potential range, -0.2 to 0.8V for various current rates (1 – 50 mA/cm²)

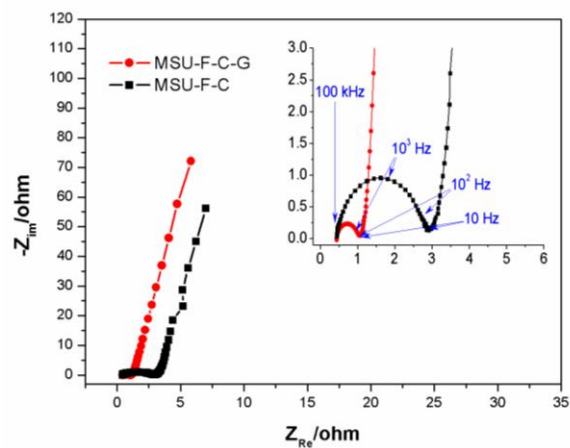


Figure S5. Nyquist plots of MSU-F-C and MSU-F-C-G at 0.2 V. (Inset : magnified view.)

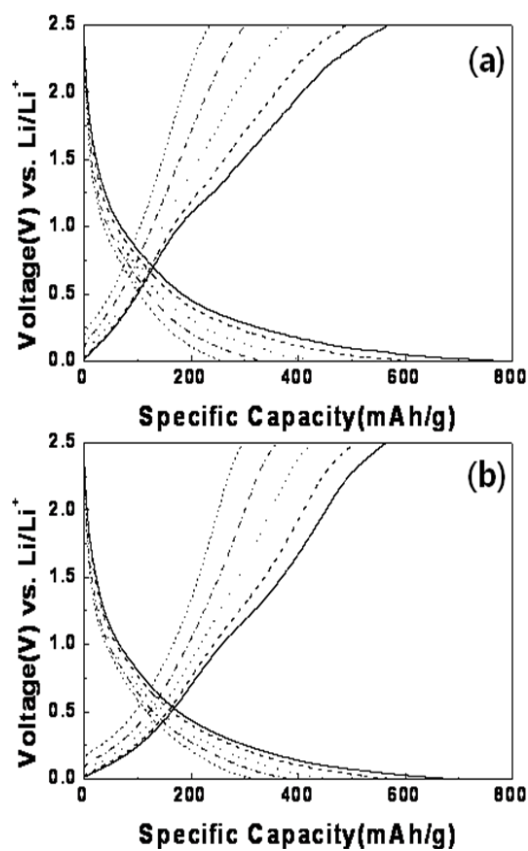


Figure S6. Change of the galvanostatic charge-discharge patterns of the (a) MSUF-F-C and (b) MSU-F-C-G anodes according to an applied current of 0.1 (solid), 0.2 (dashed), 0.5 (dotted), 1 (dash-dotted) and 2 C (short-dashed).

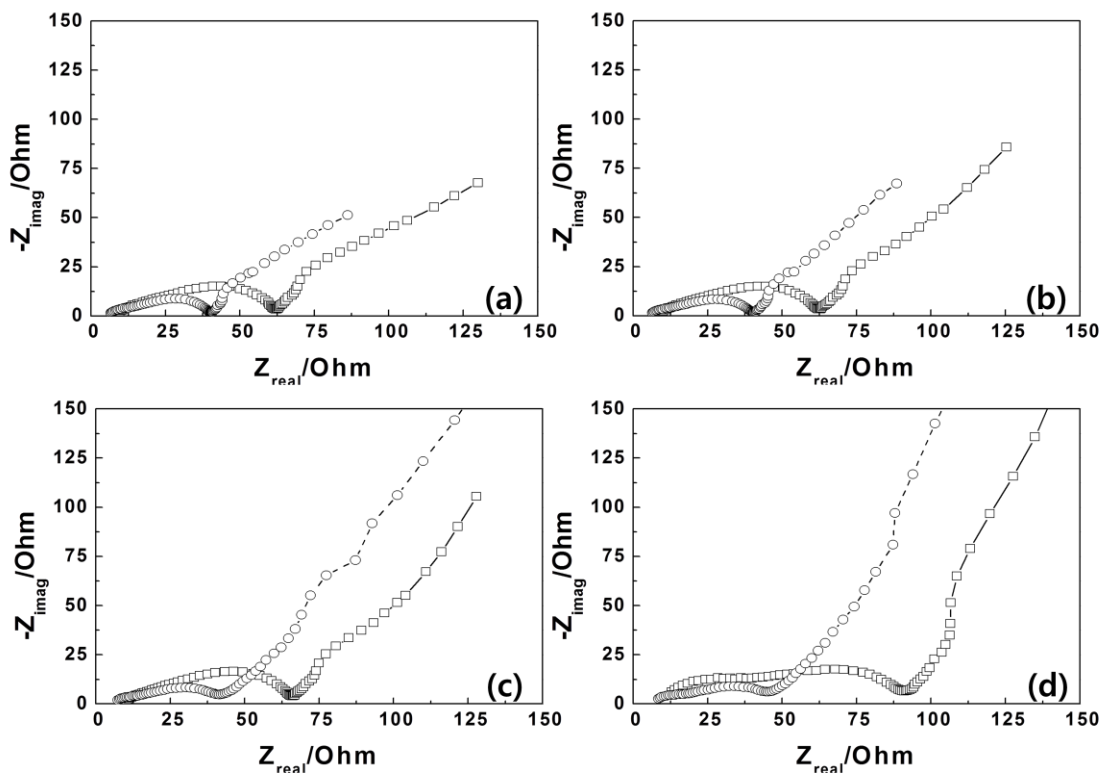


Figure S7. Electrochemical impedance spectra of the MSU-F-C (rectangles) and MSU-F-C-G (circles) anodes expressed as Nyquist plots according to measuring potentials of (a) 0, (b) 0.5, (c) 1.0 and (d) 2.0 V vs. Li/Li^+ .